I.A.U
Karaj branch

Journal of
A p p l ied
C hemical
R esearch
jacr.kiau.ac.ir

Journal of Applied Chemical Research, 11, 3, 28-45 (2017)

Solvent Effect on the Molecular Structure, Chemical Reactivity and Spectroscopy Properties of Z-Ligustilide: A Main Active Component of Multitude Umbelliferae Medicinal Plants

Mahmoud Osanloo[1], Reza Ghiasi*[2]

[1]Department of Medical Nanotechnology, School of Advanced technologies in Medicine, Tehran University of Medical Sciences, Tehran, IRAN

[2]Department of Chemistry, East Tehran branch, Islamic Azad university, Qiam Dasht, Tehran, Iran

(Received 03Dec. 2016; Final version received 11Mar. 2017)

Abstract

In this investigation, the structural, electronic properties, ^{13}C and ^{1}H NMR parameters and first hyperpolarizability of Z-Ligustilide were explored. As well, the solvent effect on structural parameters, frontier orbital energies, electronic transitions, and^{13}C and ^{1}H NMR parameters was illustrated based on Polarizable Continuum Model (PCM).These consequences specify that the polarity of solvents participates on the structures and spectroscopic properties of Z-Ligustilide.NBO analysis was used to examining of the hybridation of atoms, atomic charges and their second order stabilization energy within the molecule.

Keywords: *Z-Ligustilide, Frontier orbital analysis, ^{1}H and ^{13}C NMR calculations, NBO analysis.*

**Corresponding author:* *Reza Ghiasi,Department of Chemistry, East Tehran branch, Islamic Azad University, Qiam Dasht, Tehran, Iran. Email:rghiasi@iauet.ac.ir.*

Introduction

Z-Ligustilide(LIG) or 3-butylidene-4,5-dihydrophthalideis the main active component of multitudeUmbelliferae medicinal plants [1-3]. Two important plants in traditional Chinese and Iranian medicine are Radix Angelica Sinensis (RAS) and Kelussiaodoratissima Mozaffarian (KO) that practicable to relieve various diseases. LIGis one of the major ingredients of the essential oils (EO) of RAS and KO [4-7]. LIG performances a variety of biological and pharmacological activities, include reduced vascular resistance, lead to increase blood flow and increase microcirculation to pull up cardiovascular disease.

Also, LIG has a protective effect against ischemic brain injury effected by the defeat of regular blood supply to brain in the CNS (central nervous system) [4, 8]. LIG can increase the activity of antioxidant enzymes such as glutathione peroxidase and superoxide dismutase and enhancing anti-oxidant effects by decrease in malondialdehyde, a yield of lipid peroxidation, and also, had neuro protective effects on diseases deal with cerebral ischemia. Treatment with LIG could foster an anti-apoptotic result specifically via up-regulation of Bcl-2 and down-regulation of Bax and caspase-3that reduces cerebral infarct volumes after focal cerebral ischemia in rats and significantly improve behavioral deficits [4, 9-15]. Anti-inflammatory effects innanoemulsion form, toxicity (LD50 = 10.23 μg/adult) against *Sitophilus*. zeamais (maize weevil) as well as the phytotoxic effect to Lemna paucicostata are other applications of it in former researches [16-18].

LIG is a volatile and unstable compound and it can degrade into other compounds of phthalides through some chemical reactions (oxidation, isomerization or dimerization). Such properties causes limit its study and good clarify its application.To better explore to control its quality and the best storage conditions, many researchers have been done. Affected key factors including pH, light, temperature, antioxidants, co-solvents, and manner of stabilization have been investigated [19-21].

In this paper, we illustrate the structural, vibrational spectrum, electronic properties, ^{13}C and ^{1}H NMR parameters and electronic spectrum of Z-Ligustilide in the M062X/6-311G(d,p) level.

Experimental

All calculations were carried out with the Gaussian 03 suite of program [22]. The standard 6-311G(d,p) basis set [23-26] and the hybrid functional of Truhlar and Zhao (M062X) [27] are used for optimization of molecule.A vibrational analysis was performed at each stationary point found, that confirm its identity as an energy minimum.The population analysis has also been performed by the natural bond orbital method [28] using NBO program [29] under Gaussian 2003 program package in the M062X/6-311G(d,p) level of theory. Gauss-Sum 2.2 program [30] has been used to calculate group contributions to the molecular orbitals (HOMO and LUMO) and prepare the density

of states (DOS) spectrum in the M062X/6-311G(d,p) level of theory.NMR calculations are calculated using the Gauge independent atomic orbital (GIAO) [31] method at the M062X /6-311G(d,p) level of theory.The electronic spectra for the studied complexes were calculated by TD-DFT [32] using the same hybrid functionals and basis set as used for the optimization. The 20 lowest excitation energies were calculated.

Results and discussion

Energy

Figure 1 presents the molecular structure of Ligustilide molecule. Absolute energy, Zero point vibration energy, energy, Molar capacity at constant volume, entropy, dipole moment of Z-Ligustilide molecule are reported in Table 1. The energies of Ligustilide molecule in gas phase and in different media by using the PCM model are gathered in Table 2. E_T is the total energy and ΔE_{solv} is the stabilization energy by solvents, the relative energy of the title compound in a solvent to that in the gas phase.

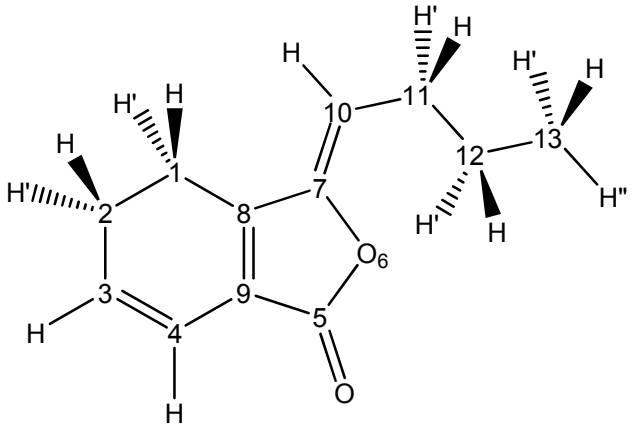

Figure 1. The structure of Ligustilide molecule.

Table 1. Absolute energy, Zero point vibration energy, energy, Molar capacity at constant volume, Entropy, Dipole moment of Z-Ligustilide molecule.

Parameters			
Absolute energy (Hartree)		-616.0292371	
Zero point vibration energy (Joules/Mol)		618849.3	
Rotational constants(GHZ)	1.42239	0.39558	0.31405
Rotational temperature (K)	0.06826	0.01898	0.01507
Energy (kcal/Mol)			
Translational		0.889	
Rotational		0.889	
Vibrational		154.300	
Total		156.077	
Molar capacity at constant volume (Cal/Mol-Kelvin)			
Translational		2.981	
Rotational		2.981	
Vibrational		43.231	
Total		49.193	
Entropy (Cal/Mol-Kelvin)			
Translational		41.633	
Rotational		31.876	
Vibrational		41.910	
Total		115.418	
μ_x		1.2731	
μ_y		-4.9100	
μ_z		-0.1186	
Dipole moment (Debye)		5.0738	

From Table 2, we can see that the calculated energy is dependent on the size of the dielectric constant of solvents. In the PCM model, the energies E_T decrease with the increasing dielectric constants of solvents. On the other hand, ΔE_{solv} values indicate to increasing of stability in more polar solvents. This is because a dipole in the molecule will induce a dipole in the medium, and the electric field applied to the solute by the solvent (reaction) dipole will in turn interact with the molecular dipole to lead to net stabilization. This suggests that the Ligustilide molecule has more stability in polar solvent rather than in the gas phase. There is a good correlation between dielectric constants and E_{solv} (Figure 2).

Table 2. Absolute energy (E, Hartree), solvation energy (**E_{solv}**,kcal/mol), solvent dielectric constant, Z-Ligustilide molecule in solution phases.

	ε	**E**	**E_{solv}**	**μ**
Gas	-	-616.0292	-	5.07
Chloroform	4.71	-616.0357	-4.03	6.48
Chlorobenzene	5.70	-616.0361	-4.33	6.59
THF	7.43	-616.0367	-4.68	6.72
Methylenechloride	8.93	-616.0370	-4.88	6.80
Quinoline	9.16	-616.0371	-4.91	6.81
Isoquinoline	11.00	-616.0373	-5.08	6.88

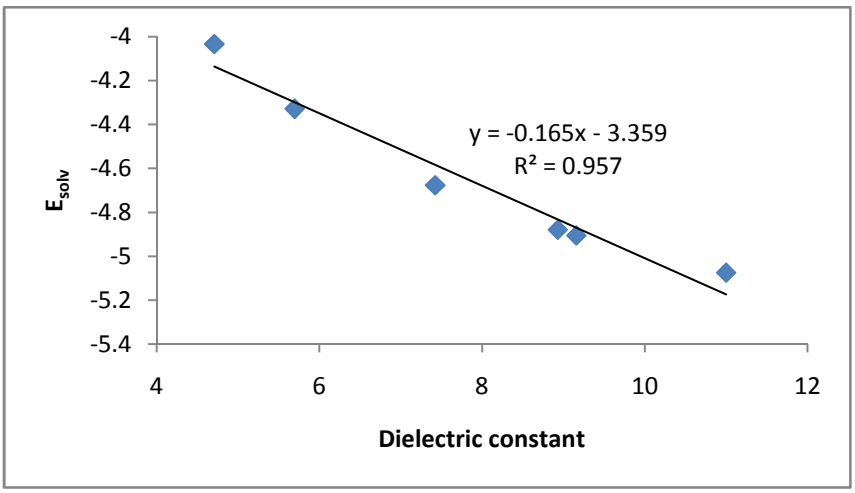

Figure 2. Correlation between salvation energy (E_{solv}) and dielectric constant.

Dipole moments

Dipole moment values of Ligustilide in gas phase and in different media by using the PCM model are listed in Table 2. These values show the solvent effect on the stabilization energy is in parallel with that on the dipole moment of the solute. There is a good linear relationship between the solvent stabilization energies and the dipole moments of Ligustilide in the set of solvents with the correlation coefficient equals to 1.00. Namely, there is the larger the dipole moment of solute, and the higher the stabilization energy in the stronger the solvent polarity. Also, there is a good correlation between dipole moment and dielectric constant with the correlation coefficient is 0.959 (Figure 3).

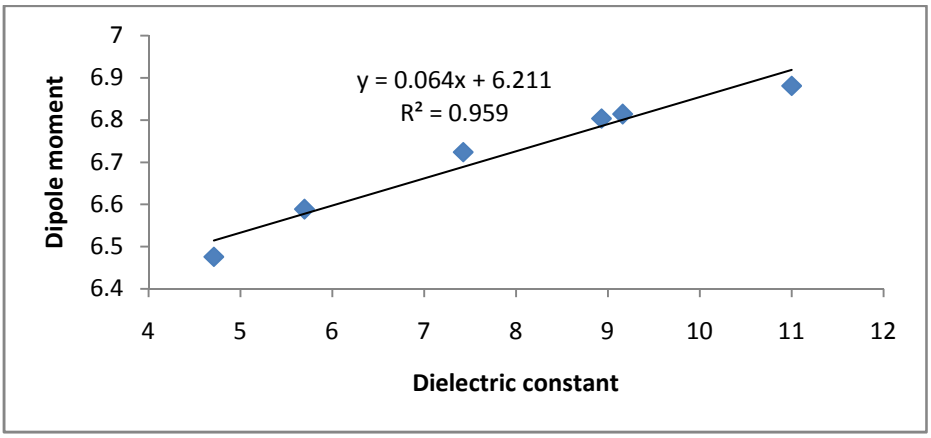

Figure 3. Correlation between dipole moment and dielectric constant.

Frontier orbitals energy

The influence of solvent nature is reflected not only in the geometric parameters of the molecules, but also in the energies of frontier orbitals. It is well-known that the frontier orbitals energy and HOMO-LUMO gap values are closely related to the optical and electronic properties. The inclusion of solvation effects leads also to changes on the molecular orbital energies (Table 3). In solution, HOMO is stabilized, with respect to the corresponding values in vacuum, but LUMO is destabilized.A good linear relation is seen between frontier orbitals energy and dielectric constants (R^2= 0.999, 0.996, for HOMO and LUMO, respectively).

Table 3. Frontier orbital energies (in a.u), HOMO-LUMO gap (in eV), Hardness (in eV), softness (in eV^{-1}), chemical potential (in eV), electrophilicity (in eV) for Z-Ligustilide molecule in vacuum and solution phases.

Molecule	HOMO	LUMO	ΔE	η	S	μ	ω
Gas	-0.2727	-0.0440	6.222	3.111	0.321	-4.309	2.984
Chloroform	-0.2728	-0.0453	6.191	3.096	0.323	-4.327	3.024
Chlorobenzene	-0.2728	-0.0454	6.189	3.094	0.323	-4.330	3.029
THF	-0.2729	-0.0456	6.186	3.093	0.323	-4.333	3.035
Methylenechloride	-0.2729	-0.0457	6.184	3.092	0.323	-4.335	3.039
Quinoline	-0.2729	-0.0457	6.184	3.092	0.323	-4.335	3.039
Isoquinoline	-0.2730	-0.0458	6.182	3.091	0.324	-4.337	3.042

The HOMO-LUMO gaps in solvated media are higher than the corresponding values computed in vacuum. A good linear relation is seen between HOMO-LUMO gaps and dielectric constants (R^2= 0.998).To get insight into the influence of the optical and electronic properties, the distributions of the frontier orbitals for these molecules are investigated, and their sketches are plotted in Figure 4(a). Molecular orbital analysis show that HOMO and LUMO are of the π characteristics as visualized in Figure 4(a) for Ligustilide.

In addition, the total density of states (DOS) of Ligustilide has been presented in Figure 4(b) to more easily and vividly observe the varieties of the HOMOs, LUMOs, and energy gaps.

As well as, the study of effect of the solvent on the chemical potential values shows that increasing of these values with increasing of dielectric constants. On the other hand, electrophilicity values decrease with increasing of dielectric constants. As seen as Table 3, there is a good correlation between chemical potential and electrophilicity values with dielectric constants.

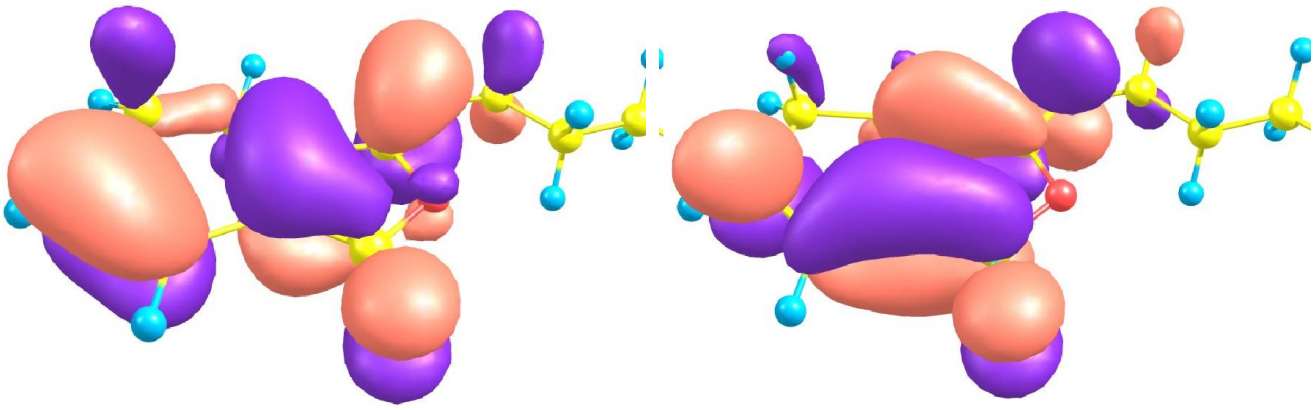

HOMO LUMO

(a)

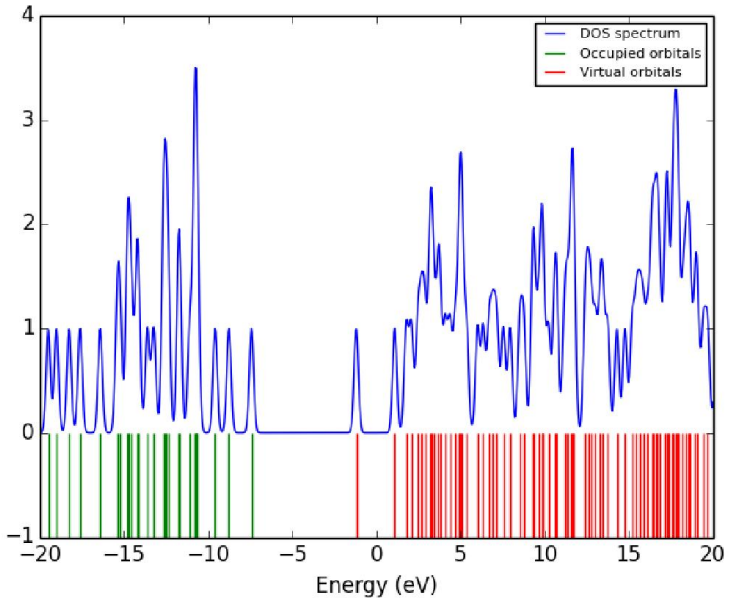

Figure 4.(a) The plots of frontier orbitals and (b) Density of states (DOS) diagram.

Structural properties

The Z-Ligustilide molecule contains one six membered ring fused with a five membered ring along with one group attached to C7 atom. The optimized structural parameters bond length and bond angle for the thermodynamically preferred geometry of Z-Ligustilide determined at M062X method using 6–311G(d,p) basis set are reported in Table 4.

Table 4. CC and CO bond lengths (in Å) for Z-Ligustilide molecule in vacuum and solution phases.

Molecule	C1C2	C2C3	C3C4	C4C9	C9C5	C5O5	C5O6	O6C7	C7C8	C1C8	C8C9	C7C10	C10C11	C11C12	C12C13
Gas	1.5383	1.5138	1.3373	1.4540	1.4744	1.1904	1.3853	1.3814	1.4566	1.4951	1.3443	1.3349	1.4985	1.5279	1.5264
Chloroform	1.5382	1.5132	1.3379	1.4550	1.4697	1.1963	1.3793	1.3867	1.4550	1.4946	1.3463	1.3347	1.4975	1.5275	1.5266
Chlorobenzene	1.5382	1.5132	1.3379	1.4551	1.4693	1.1968	1.3790	1.3872	1.4548	1.4945	1.3465	1.3347	1.4974	1.5275	1.5266
THF	1.5382	1.5131	1.3380	1.4551	1.4689	1.1973	1.3784	1.3877	1.4547	1.4945	1.3467	1.3347	1.4973	1.5274	1.5266
Methylenechloride	1.5382	1.5131	1.3380	1.4552	1.4686	1.1976	1.3782	1.3880	1.4546	1.4944	1.3468	1.3347	1.4972	1.5274	1.5266
Quinoline	1.5382	1.5131	1.3380	1.4552	1.4686	1.1976	1.3782	1.3880	1.4545	1.4944	1.3468	1.3347	1.4972	1.5274	1.5266
Isoquinoline	1.5382	1.5131	1.3381	1.4552	1.4683	1.1979	1.3779	1.3883	1.4545	1.4944	1.3469	1.3347	1.4972	1.5274	1.5266

CC bond lengths

In the title molecule, the calculated C(3)C(4), and C(7)C(10) bond lengths are 1.337, and 1.335 Å, respectively. On the other hand, the calculated C(1)C(2), C(2)C(3), C(4)C(9), C(1)C(8), C(5)C(9) and C(7)C(8) bond lengths are 1.538, 1.514,1.454, 1.495, 1.474,and 1.457 Å, respectively. The extension of these bond lengths rather than C(3)C(4), and C(7)C(10) bonds confirm the presence of double bond character in C(3)C(4), C(8)C(9) and C(7)C(10) bonds. the calculated C(5)O(5), C(5)O(6), and C(7)O(6) bond lengths are 1.190, 1.385,and 1.381 Å, respectively.

The fused ring bond C(8)C(9) is 1.344 Å.

The calculated C(10)C(11), C(11)C(12), and C(12)C(13) bond lengths are 1.498, 1.528,and 1.526 Å, respectively.

CO bond lengths

The shorting of C(5)O(5) bond length rather than C(5)O(6), and C(7)O(6) bonds is compatible with the existence of double bond character in C(5)O(5) bond.

CH bond lengths

The C(3)H(3) and C(4)H(4) bond lengths are of the order of 1.084 and 1.083 Å, respectively.

The comparison of the bond lengths in vacuum phase and solution phase show the shorting the C1C2, C2C3, C9C5, C5O6 , C7C8, C7C10, C10C11, and C11C12 bonds. On the other hand, the C3C4, C4C9, C5O5, C7O6, C1C8, and C12C13 lengthen in solution phase.

Local reactivity descriptors

Nucleophilic reactivity descriptors (f_k^-, s_k^-, ω_k^-) for Z-Ligustilide, using Mulliken atomic charges are gathered in Table 5. The maximum values of the local nucleophilic reactivity descriptors (f_k^-, s_k^-, ω_k^-) at C10, and O5 indicate that these sites are susceptible to electrophilic attack.

Electrophilic reactivity descriptors (f_k^+, s_k^+, ω_k^+)[33], using Mulliken atomic charges are listed in Table 5. The maximum values of local electrophilic reactivity descriptors (f_k^+, s_k^+, ω_k^+) of Z-Ligustilide at C10 and O5 atoms signify that these sites are more disposed to nucleophilic attack.

Table 5. Nucleophilic reactivity descriptors (f_k^-, s_k^-, ω_k^-), electrophilic reactivity descriptors descriptors (f_k^+, s_k^+, ω_k^+)for Z-Ligustilide molecule.

	f^+	f^-	f^0	s^+	s^-	s^0	ω+	ω^-	ω^0
C1	0.0001	-0.0057	-0.0028	0.0000	-0.0018	-0.0009	0.0003	-0.0171	-0.0084
C2	-0.0113	-0.0187	-0.0150	-0.0036	-0.0060	-0.0048	-0.0338	-0.0559	-0.0449
C3	0.0966	0.0898	0.0932	0.0310	0.0289	0.0300	0.2882	0.2679	0.2780
C4	0.0529	0.0115	0.0322	0.0170	0.0037	0.0104	0.1578	0.0344	0.0961
C5	0.0398	0.0813	0.0606	0.0128	0.0261	0.0195	0.1189	0.2425	0.1807
O5	0.0945	0.1131	0.1038	0.0304	0.0363	0.0334	0.2819	0.3373	0.3096
O6	0.0345	0.0418	0.0381	0.0111	0.0134	0.0123	0.1029	0.1247	0.1138
C7	-0.0019	-0.0579	-0.0299	-0.0006	-0.0186	-0.0096	-0.0057	-0.1728	-0.0893
C8	0.0307	0.0852	0.0580	0.0099	0.0274	0.0186	0.0916	0.2543	0.1729
C9	0.0246	0.0047	0.0146	0.0079	0.0015	0.0047	0.0734	0.0140	0.0437
C10	0.1307	0.1480	0.1393	0.0420	0.0476	0.0448	0.3900	0.4415	0.4158
C11	-0.0296	0.0353	0.0029	-0.0095	0.0114	0.0009	-0.0884	0.1054	0.0085
C12	-0.0049	-0.0471	-0.0260	-0.0016	-0.0151	-0.0084	-0.0148	-0.1406	-0.0777
C13	0.0089	0.0139	0.0114	0.0029	0.0045	0.0037	0.0266	0.0414	0.0340

Vibrational analysis

The Ligustilide molecule possesses C1 point group symmetry. This compound consists of 28 atoms, which construct 78 normal modes of fundamental vibrations.

CH_3

The stretching vibrations of CH_3 are expected in the range 2900–3050 cm^{-1}[34, 35]. The band at 3045.26 cm^{-1} result from symmetric stretching $\upsilon_s(CH_3)$ in which all three of the C-H bonds expand and contract in-phase.

C=O

The band at 1926.43 cm^{-1} attribute to stretching of C(5)=O(5) bond.

CH_2

The bands at 3014.45 cm^{-1} and 3039.89 cm^{-1} can be assigned to symmetric and asymmetric stretching of CH bonds of $C(11)H_2$, respectively.

The band at 3028.25 cm^{-1} result from symmetric stretching of C(1)H'(1) and C(2)H(2) bonds, all together. The band at 3037.25 cm^{-1} belong to asymmetric stretching of C(1)H'(1) and C(2)H(2) bonds, at once.The band at 3103.70 cm^{-1} result from symmetric stretching of C(1)H (1) and C(2)H'(2) bonds, all together. The band at 3107.36 cm^{-1} owing to asymmetric stretching of C(1)H(1) and C(2)H'(2) bonds, all together.The band at 3078.86 cm^{-1} is due to symmetric stretching of CH bonds of $C(12)H_2$.

CH

The band at 3212.26 cm^{-1} corresponds to symmetric stretching of CH bonds of C(3)H(15) and C(4)H(16), all together. The band at 3190.46 cm^{-1} describes asymmetric stretching of CH bonds of C(3)H(15) and C(4)H(16).The band at 3167.73 cm^{-1} corresponds to stretching of CH bonds of C(11)H(11).

C=C

The bands at 1683.34 cm^{-1} and 1718.98 cm^{-1} owing to symmetric and asymmetric stretching of C3=C4 and C8=C9 bonds, respectively. Concurrently, two C=C bonds expand or contract in symmetric stretching. But, these C=C bonds expand and contract in asymmetric stretching at the same time.The calculated wavenumbers at 1771.14 cm^{-1} describes the presence of the C7=C10.

Electronic spectra

We investigated the most intense electronic transition (λ_{max}) of molecule. The wavelength, oscillator strength and the composition of the transitions obtained by TD-DFT calculations are given in Table 6. Theoretical calculations reveal that, in Ligustilide molecule HOMO $\rightarrow$LUMO transition makes the major contribution in this electronic transition. Addition of solvation effects directs to changes on λ_{max} (Table 6). In solution, the λ_{max} is red-shifted with respect to the corresponding values in vacuum.

Table 6. The wavelength, oscillator strengths, the composition of the maximum electronic transitions for Z-Ligustilide molecule in vacuum and solution phases.

	λ_{max} (nm)	f
Gas	298.65	0.3453
Chloroform	308.43	0.4079
Chlorobenzene	309.49	0.4169
THF	308.48	0.3977
Methylenechloride	308.86	0.3994
Quinoline	302.66	0.3163
Isoquinoline	302.80	0.3154

Hyperpolarizability

Hyperpolarizability (β) reported here is defined as:

$$\beta_{tot} = (\beta_x^2 + \beta_y^2 + \beta_z^2)^{\frac{1}{2}}$$

Where

$$\beta_i = \frac{1}{3} \sum_{k=x,y,z} (\beta_{ikk} + \beta_{kik} + \beta_{kki}); i = x, y, z$$

Theoretical investigation assists a fundamental role in comprehending of the structure-property correlations, which is able to maintain designing of novel NLO chormophores. The electrostatic first hyperpolarizability (β_{tot}) and dipole moment (μ) of Z-Ligustilide have been calculated in both gas phase and various solvents. As can be seen from Table 7, it is obvious that largest β_{tot} values are found in higher polartiity. Also, β_{tot} values increase from vacuum phase to different solvents. the first hyperpolarizability of the title compound dependents on the dielectric constant of the media and the Onsager function [36], that is distinctive for a dipolar reaction field interaction in the salvation process [37-39]. The corresponding equations are:

$$10^{30}\beta_{tot} = 0.0777\ \varepsilon + 5.3921;\ R^2 = 0.9581$$

$$10^{30}\beta_{tot} = 6.2211\ \frac{(\varepsilon-1)}{(2\varepsilon+1)} + 3.4929;\ R^2 = 0.9998$$

Table 7. β components and β_{tot} values for for Z-Ligustilide molecule in vacuum and solution phases.

	Gas	**Chloroform**	**Chlorobenzene**	**THF**	**Methylenechloride**	**Quinoline**	**Isoquinoline**
β_{XXX}	465.00	761.83	786.58	816.28	834.05	836.32	851.42
β_{XXY}	41.90	68.65	70.48	72.50	73.65	73.79	74.72
β_{XYY}	-12.03	-62.73	-69.50	-78.19	-83.65	-84.36	-89.17
β_{YYY}	-52.69	-53.28	-52.58	-51.65	-51.03	-50.94	-50.37
β_{XXZ}	-7.82	-16.36	-17.46	-18.92	-19.81	-19.92	-20.73
β_{XYZ}	-5.73	-14.49	-15.34	-16.41	-17.04	-17.12	-17.67
β_{YYZ}	-8.29	-15.07	-15.74	-16.52	-17.02	-17.08	-17.52
β_{XZZ}	-29.45	-46.37	-48.03	-50.06	-51.28	-51.44	-52.49
β_{YZZ}	-70.58	-109.49	-113.15	-117.62	-120.31	-120.66	-122.97
β_{ZZZ}	-0.90	-2.79	-2.81	-2.87	-2.89	-2.90	-2.91
β_{tot}	3.73×10^{-30}	5.71×10^{-30}	5.85×10^{-30}	6.01×10^{-30}	6.11×10^{-30}	6.12×10^{-30}	6.20×10^{-30}
$\beta_{tot}\times10^{30}$	3.73	5.71	5.85	6.01	6.11	6.12	6.20
β_X	3.66×10^{-30}	5.64×10^{-30}	5.78×10^{-30}	5.94×10^{-30}	6.04×10^{-30}	6.05×10^{-30}	6.13×10^{-30}
β_Y	-7.03×10^{-31}	-8.13×10^{-31}	-8.23×10^{-31}	-8.40×10^{-31}	-8.40×10^{-31}	-8.45×10^{-31}	-8.50×10^{-31}
β_Z	-1.47×10^{-31}	-2.96×10^{-31}	-3.11×10^{-31}	-3.30×10^{-31}	-3.40×10^{-31}	-3.45×10^{-31}	-3.60×10^{-31}

Thermodynamic parameters

Thermochemical analysis is studied for Z-Ligustilide. According to the statistical thermodynamic principle, heat capacities (C_v ,m in cal K^{-1} mol^{-1}), entropies (S, in cal K^{-1} mol^{-1}), and enthalpies (H, in kcal mol^{-1}) in ranging from 100 to 10000 K were obtained and are gathered in Table 8. As it is obvious from Table 8, the C_v, S, and H thermodynamic functions of Z-Ligustilide with the increase of temperature. The reason for this is that the vibrational movement is invigorated at the higher temperature and makes more contributions to the thermodynamic functions, although the main contributions are due to the translation and rotation of the molecules at the lower temperature. The relationships between the thermodynamic functions and the temperature in 100–1000 K, are expressed as:

$G = -1 \times 10^{-7} T^2 - 1 \times 10^{-4} T - 615.79;$ $R^2 = 1.0000$

$H = 9 \times 10^{-8} T^2 + 3 \times 10^{-5} T - 615.8;$ $R^2 = 0.9996$

$C_v = -7 \times 10^{-5} T^2 + 0.1882 T + 1.0201;$ $R^2 = 0.999$

$S = -4 \times 10^{-5} T^2 + 0.2006 T + 59.007;$ $R^2 = 1.0000$

Table 8. Thermodynamic parameters for Z-Ligustilide molecule in various temperatures.

T	G(a.u)	H(a.u)	S(Cal/mol.K)	C_v(Cal/mol.K)
100	-615.8036	-615.7911	78.16	21.01
200	-615.8177	-615.7864	98.19	34.39
300	-615.8347	-615.7794	115.74	49.48
400	-615.8545	-615.7700	132.67	64.82
500	-615.8770	-615.7582	149.08	78.38
600	-615.9020	-615.7445	164.76	89.70
700	-615.9295	-615.7291	179.62	99.07
800	-615.9592	-615.7124	193.64	106.87
900	-615.9911	-615.6945	206.85	113.44
1000	-616.0251	-615.6756	219.31	119.01

^{1}H and ^{13}C NMR chemical shifts

The theoretical and experimental ^{1}H and ^{13}C NMR chemical shifts of the Z-Ligustilide are listed in Table 9. Relative chemical shifts are calculated by using the corresponding TMS shielding estimated in advance at the same theoretical level as the reference.GIAO method has been used for NMR calculations.

^{1}H NMR

The trend of proton signals in Z-Ligustilide is: H4>H3>H10>H1>H2>H11>H12>H13. In the basis of this trend the chemical shift of H4, H3, and H10 are higher than otherhydrogen atoms. Consequently, the electronic charge densities around the H4, H3, and H10 are lower than other hydrogen atoms. On the other hand, the chemical shift values of H1, H2, H11, and H13 decrease in

solution phase rather than vacuum phase. For other hydrogen atoms, these values increase in solution phase.

^{13}C NMR

The signal of carbonyl carbon atom (C5) wasdetected at 172.63 ppm, in gas phase.This atom has larger chemical shift than the other molecule carbon atoms owing to electronegativity of oxygen atom. The relations between the experimental and calculated chemical shifts are examined in gas and solution phases and correlation coefficients are reported in Table 9.These values indicate a good correlation between predicted and observed proton and carbon chemical shifts. The study of solvent effect on the ^{13}C NMR chemical shift exhibits the chemical shift values of H1, H2, H12, and H13 decrease in solution phase rather than vacuum phase. For other carbon atoms, these values increase in solution phase.

Table 9. ^{1}H and ^{13}C NMR chemical shifts for Z-Ligustilide molecule in vacuum and solution phases (in ppm, respect to TMS)

^{1}H NMR

	H1	H2	H3	H4	H10	H11	H12	H13	R^2(exp)
Exp	2.60	2.46	6.00	6.29	5.22	2.37	1.5	0.95	-
Gas	2.21	2.08	6.47	6.98	5.32	2.03	1.95	0.79	0.979
Chloroform	2.34	2.17	6.65	6.94	5.68	2.12	1.84	0.80	0.988
Chlorobenzene	2.35	2.17	6.66	6.93	5.71	2.13	1.83	0.80	0.989
THF	2.36	2.18	6.68	6.93	5.74	2.14	1.81	0.80	0.989
Methylenechloride	2.37	2.18	6.69	6.92	5.76	2.15	1.81	0.80	0.989
Quinoline	2.37	2.18	6.69	6.92	5.77	2.15	1.81	0.80	0.989
Isoquinoline	2.38	2.19	6.70	6.92	5.78	2.15	1.80	0.80	0.990

^{13}C NMR

	C1	C2	C3	C4	C5	C7	C8	C9	C10	C11	C12	C13	R^2(exp)
EXP	18.30	22.20	129.90	116.80	167.50	147.00	148.40	123.70	112.90	28.00	22.00	13.60	-
Gas	16.81	21.60	146.25	136.02	172.63	161.86	165.97	139.12	122.92	32.76	17.57	12.29	0.994
Chloroform	17.06	21.71	149.67	134.43	176.54	161.73	169.71	138.09	127.73	33.04	18.07	12.28	0.995
Chlorobenzene	17.08	21.72	149.92	134.31	176.81	161.71	170.02	137.98	128.14	33.07	18.11	12.28	0.995
THF	17.11	21.74	150.22	134.16	177.12	161.68	170.38	137.86	128.63	33.09	18.16	12.27	0.995
Methylenechloride	17.13	21.74	150.39	134.07	177.30	161.67	170.60	137.79	128.92	33.11	18.19	12.27	0.995
Quinoline	17.13	21.75	150.41	134.06	177.33	161.66	170.63	137.78	128.95	33.11	18.19	12.27	0.995
Isoquinoline	17.15	21.75	150.55	133.98	177.48	161.65	170.82	137.71	129.20	33.13	18.22	12.27	0.995

Natural Bond Orbital (NBO) analysis

Natural Bond Orbital (NBO) analysis gives a helpful method for investigation of attractive features of molecular structure. NBO theory lets the determination of the hybridization of atomic lone pairs and of the atoms included in bond orbitals. The calculated natural orbital occupancy (number of electron, or ‘‘natural population” of the orbital) and hybridization of C-C and C-O bonds of title molecule have been tabulated in Table10.

Table 10. Occupancy of natural orbitals (NBOs) and hybrids of C-C and C-O bonds in Z-Ligustilide molecule.

NBO	occupancy	Hybride
σ(C1- C2)	1.97783	0.7123 $(sp\ 2.58)_{C1}$ + 0.7019 $(sp\ 2.57)_{C2}$
σ(C1 - C8)	1.97546	0.7008 $(sp\ 2.50)_{C1}$ + 0.7134 $(sp\ 1.92)_{C8}$
σ(C2 - C3)	1.98090	0.7146 $(sp\ 2.50)_{C2}$ + 0.6995 $(sp\ 2.06)_{C3}$
σ(C3 - C4)	1.98159	0.7011 $(sp\ 1.58)_{C3}$ + 0.7131 $(sp\ 1.61)_{C4}$
π(C3 - C4)	1.91804	0.6992 $(p99.99)_{C3}$ + 0.7149 $(p99.99)_{C4}$
σ(C 4 - C5)	1.97182	0.6935 $(sp\ 2.08)_{C4}$ + 0.7205 $(sp\ 1.82)_{C5}$
σ(C 8 - C 9)	1.96562	0.7094 $(sp\ 1.81)_{C8}$+ 0.7048 $(sp\ 1.91)_{C9}$
π(C8 - C9)	1.81172	0.7315 $(p99.99)_{C8}$ + 0.6818 $(p\ 1.00)_{C9}$
σ(C9 - C5)	1.97582	0.7251 $(sp\ 2.47)_{C9}$ + 0.6886 $(sp\ 1.55)_{C5}$
σ(C8 - C 7)	1.96753	0.7108 $(sp\ 2.19)_{C8}$ + 0.7034 $(sp\ 1.92)_{C7}$
σ(C7 - O6)	1.98686	0.5660 $(sp\ 3.33)_{C7}$ +0.8244 $(sp\ 2.08)_{O6}$
σ(C 7 - C10)	1.97803	0.7151 $(sp\ 1.35)_{C7}$ +0.6990 $(sp\ 1.60)_{C10}$
π(C 7 - C10)	1.87071	0.7146 $(p\ 1.00)_{C7}$ +0.6995 $(p\ 1.00)_{C10}$
σ(O6 - C 5)	1.98931	0.8349 $(sp\ 2.44)_{O6}$ +0.5504 ($sp\ 2.90)_{C5}$
σ(C 5 - O5)	1.99494	0.5886 $(sp\ 1.87)_{C5}$ + 0.8084 $(sp\ 1.29)_{O5}$
π(C 5 - O5)	1.98194	0.5594 $(p\ 1.00)_{C5}$ + 0.8289 $(p\ 1.00)_{O5}$
σ(C 10 - C11)	1.97874	0.7096 $(sp\ 1.82)_{C10}$ +0.7046 $(sp\ 2.51)_{C11}$
σ(C11 -C 12)	1.98151	0.7165 $(sp\ 2.35)_{C11}$ +0.6975 $(sp\ 2.61)_{C11}$
σ(C12 - C13)	1.98492	0.7090 $(sp\ 2.58)_{C12}$+ 0.7053 $(sp\ 2.29)_{C13}$

Table 11 reports the calculated second order interaction energies E(2) between the donor and acceptor orbitals in Ligustilide. The second order Fock matrix has been used to estimating of the donor-acceptor interactions in the NBO analysis. For each donor (i) and acceptor (j), the stabilization energy E(2) associated with the delocalization I → j is evaluated as:

$$E^{(2)}=-q_i\frac{(F_{i,j})^2}{\varepsilon_j-\varepsilon_i}$$

The larger the E(2) value denotes to the significant interaction between electron donors and electron acceptors. The title molecule exhibits maximum stabilization energy of 44.82 kJ/mol of energy through the interaction between LP (2) of O5 and σ*(O6 – C5). It could be revealed that the anti-bonding O6 – C5 electron has 30.29% of O6 character in sp2.44 hybrid and 69.71% of C5 character in sp2.90 hybrid. The sp2.44 hybrid on O6 has 70.85% p-characters and sp2.90 hybrid on C5 has 74.14% p-character. The coefficients 0.5504 and -0.8349 found are identified polarization

coefficients of O6 and C5. The extents of these coefficients illustrate the significance of the two hybrids in the formation of the bond. The other important interaction in title molecule includes the interactions of LP (2) of O6 with π*(C5-O5) and has stabilization energies 42.88 kcal/mol. The charge distribution was evaluated from the atomic charges by NBO analysis (Figure 5). In the basis of this method O5, O6, and C13 atoms are considered as more basic site.

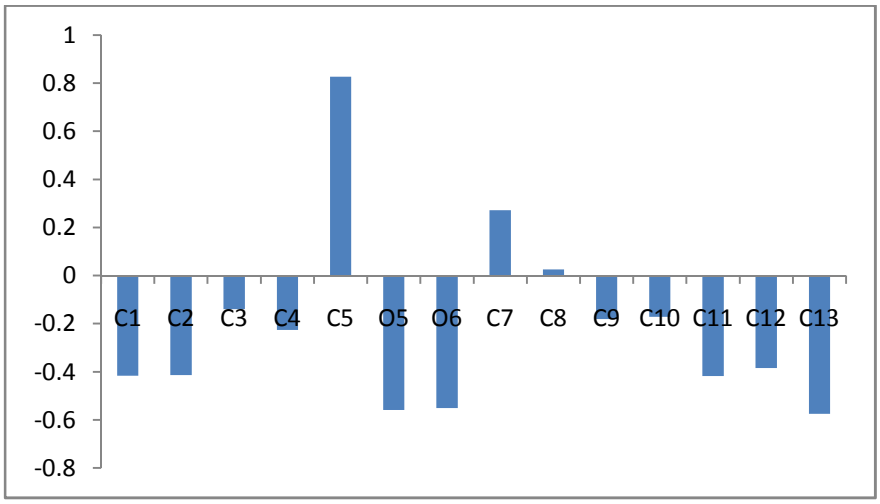

Figure 5. distribution of charges by natural charge bonding method.

Table 11. Second order perturbation theory analysis of Fock matrix in NBO basis corresponding to the intramolecular bonds of Z-Ligustilide molecule.

Donor NBO (i) →Acceptor NBO (j)	E(2) kcal/mol	E(j)-E(i) (a.u.)	F(i,j)(a.u.)
LP (2) O5 →σ*(O6 - C5)	44.82	0.72	0.163
LP (2) O 6 →π*(C7 - C10)	30.14	0.48	0.108
LP (2) O6 →π*(C 5 - O5)	42.85	0.47	0.127
π(C9 - C 8) →π*(C5 – O5)	26.19	0.40	0.093

Conclusions

In this paper, the structural and spectroscopic properties of Z-Ligustilide were studied by means of M062X method which indicated:

1. Solvation energy values indicate the increasing of stability of title molecule in more polar solvents.
2. The geometry, dipole moments, polarizability of molecule affected by solvent. With increase of the polarity of solvents the dipole moment was increased.
3. Electronic spectra analysis shows that, the most intensity of transition is assigned as HOMO →LUMO transition.

4. The experimental and calculated chemical shifts indicate a good correlation between predicted and observed proton and carbon chemical shifts.
5. The hyperpolarizability values increase from vacuum to solution phase, and are dependent on the dielectric constant of the media and the Onsager function.
6. NBO analysis show that maximum stabilization energy forthe interaction between LP (2) of O5 and σ*(O6 – C5).

References

[1] X. Kuang, J.-R. Du, Y.-S. Chen, J. Wang, Y.-N. Wang, *Pharmacology Biochemistry and Behavior,* 92 (2009).

[2] L. Mao, Z. Chaode, S. Qingmin, F. Qicheng, *Acta Pharm Sin,*14 (1979).

[3] T. Naito, Y. Ikeya, M. Okada, H. Mistuhashi, M. Maruno, *Phytochemistry,* 41 (1996).

[4] T. Chen, X. Zhu, Q. Chen, M. Ge, X. Jia, X. Wang, C. Ge, *Food chemistry*, 186 (2015).

[5] H. Vatandoost, A.S. Dehkordi, S. Sadeghi, B. Davari, F. Karimian, M. Abai, M. Sedaghat, *Experimental Parasitology*, 132 (2012).

[6] L.X. Zhao, B.C. Jiang, X.B. Wu, D.L. Cao, Y.J. Gao, *European Journal of Neuroscience*, 39 (2014).

[7] V. Mozaffarian, *Bot. Zhurn*, 88 (2003).

[8] J. Yin, C. Wang, A. Mody, L. Bao, S.-H. Hung, S.A. Svoronos, Y. Tseng, The effect of Z-Ligustilide on the mobility of human glioblastoma T98G cells (2013).

[9] X. Kuang, Y. Yao, J. Du, Y. Liu, C. Wang, Z. Qian, *Brain Research*, 1102 (2006).

[10] J. Wang, J.-r. Du, Y. Wang, X. Kuang, C.-y. Wang, *Acta Pharmacologica Sinica*, 31 (2010).

[11] D. Chen, J. Tang, N.H. Khatibi, M. Zhu, Y. Li, C. Wang, R. Jiang, L. Tu, S. Wang, *Journal of Pharmacology and Experimental Therapeutics*, 337 (2011).

[12] Y. Lu, S. Liu, Y. Zhao, L. Zhu, S. Yu, *Acta Pharmaceutica*, 64 (2014).

[13] H.-Y. Peng, J.-R. Du, G.-Y. Zhang, X. Kuang, Y.-X. Liu, Z.-M. Qian, C.-Y. Wang, *Biological and Pharmaceutical Bulletin*, 30 (2007).

[14] X.m. Wu, Z.m. Qian, L. Zhu, F. Du, W.h. Yung, Q. Gong, Y. Ke, *British journal of Pharmacology,* 164 (2011).

[15] Y. Yu, J.-R. Du, C.-Y. Wang, Z.-M. Qian, *Experimental Brain Research,* 184 (2008).

[16] Z. Ma, L. Bai, *Inflammation*, 36 (2013).

[17] S.S. Chu, G.H. Jiang, Z.L. Liu, *Journal of Chemistry*, 8 (2011).

[18] K.M. Meepagala, G. Sturtz, D.E. Wedge, K.K. Schrader, S.O. *Journal of Chemical Ecology*, 31 (2005).

[19] A.-h. ZUO, M.-c. CHENG, R.-j. ZHUO, L. WANG, H.-b. XIAO, *Journal of Pharmaceutical Sciences*, 48 (2013).

[20] F. Cui, L. Feng, J. Hu, *Drug Development and Industrial Pharmacy*, 32 (2006).

[21] H. LI, Y.-t. WANG, *Journal of Jiangxi College of Traditional Chinese Medicine*, 1 (2003).

[22] M.J. Frisch, G.W. Trucks, H.B. Schlegel, G.E. Scuseria, M.A. Robb, J.R. Cheeseman, G. Scalman, V. Barone, B. Mennucci, G.A. Petersson, H. Nakatsuji, M. Caricato, X. Li, H.P. Hratchian, A.F. Izmaylov, J. Bloino, G. Zheng, J.L. Sonnenberg, M. Hada, M. Ehara, K. Toyota, R. Fukuda, J. Hasegawa, M. Ishida, T. Nakajima, Y. Honda, O. Kitao, H. Nakai, T. Vreven, J.A. Montgomery, Jr., J.E. Peralta, F. Ogliaro, M. Bearpark, J.J. Heyd, E. Brothers, K.N. Kudin, V.N. Staroverov, R. Kobayashi, J. Normand, K. Raghavachari, A. Rendell, J.C. Burant, S.S. Iyengar, J. Tomasi, M. Cossi, N. Rega, J.M. Millam, M. Klene, J.E. Knox, J.B. Cross, V. Bakken, C. Adamo, J. Jaramillo, R. Gomperts, R.E. Stratmann, O. Yazyev, A.J. Austin, R. Cammi, C. Pomelli, J.W. Ochterski, R.L. Martin, K. Morokuma, V.G. Zakrzewski, G.A. Voth, P. Salvador, J.J. Dannenberg, S. Dapprich, A.D. Daniels, O. Farkas, J.B. Foresman, J.V. Ortiz, J. Cioslowski, D.J. Fox, in, Gaussian, Inc., Wallingford CT(2009).

[23] R. Krishnan, J.S. Binkley, R. Seeger, J.A. Pople, *J. Chem. Phys.*, 72, 650 (1980).

[24] A.J.H. Wachters, Gaussian basis set for molecular wavefunctions containing third-row atoms, *J. Chem. Phys*., 52, 1033 (1970).

[25] P.J. Hay, basis sets for molecular calculations - representation of 3D orbitals in transition-metal atoms, *J. Chem. Phys*. , 66, 4377 (1977).

[26] A.D. McLean, G.S. Chandler, ontracted Gaussian-basis sets for molecular calculations. 1. 2nd row atoms, Z=11-18, *J. Chem. Phys*. , 72, 5639 (1980).

[27] Y. Zhao, D.G. Truhla, *J. Phys. Chem*, 110, 5121 (2006).

[28] A.E. Reed, L.A. Curtiss, F. Weinhold, *Chem. Rev*., 88, 899 (1988).

[29] E.D. Glendening, A.E. Reed, J.E. Carpenter, F. Weinhold, in.

[30] N.M. O'Boyle, A.L. Tenderholt, K.M. Langer, *J. Comput. Chem*., 29, 839 (2008).

[31] K. Wolinski, J.F. Hinton, P. Pulay, *J. Am. Chem. Soc.*, 112, 8251 (1990).

[32] E. Runge, E.K.U. Gross, *Phys. Rev. Lett*. , 52, 997 (1984).

[33] W. Yang, W.J. Mortier, *J. Am. Chem. Soc*. , 108, 5708 (1986).

[34] N.P.G. Roeges, A Guide to Complete Interpretation of IR Spectra of Organic Structures, Wiles, New York(1994).

[35] N.B. Colthup, L.H. Daly, S.E. Wiberly, Introduction to Infrared and Raman Spectroscopy, Academic Press, New York(1975).

[36] L. Onsager, *J. Am. Chem. Soc.*, 58, 1486 (1936).

[37] P.C. Ray, J. Leszczynski, *Chem. Phys. Lett*., 339 (2004).

[38] K. Clays, A. Persoons, *Phys. Rev. Lett*. , 66, 2980 (1991).

[39] H. Lee, S.-Y. An, M.Cho, *J. Phys. Chem. B*, 103, 4992 (1999).